



HAL
open science

Orange peel coupling in multilayers with perpendicular magnetic anisotropy: application to (Co/Pt)-based exchange-biased spin-valves

Jérôme Moritz, F Garcia, J C Toussaint, B Dieny, J P Nozières

► To cite this version:

Jérôme Moritz, F Garcia, J C Toussaint, B Dieny, J P Nozières. Orange peel coupling in multilayers with perpendicular magnetic anisotropy: application to (Co/Pt)-based exchange-biased spin-valves. EPL - Europhysics Letters, 2004, 65, pp.123 - 129. 10.1209/epl/i2003-10063-9 . hal-03913363

HAL Id: hal-03913363

<https://hal.science/hal-03913363v1>

Submitted on 26 Dec 2022

HAL is a multi-disciplinary open access archive for the deposit and dissemination of scientific research documents, whether they are published or not. The documents may come from teaching and research institutions in France or abroad, or from public or private research centers.

L'archive ouverte pluridisciplinaire **HAL**, est destinée au dépôt et à la diffusion de documents scientifiques de niveau recherche, publiés ou non, émanant des établissements d'enseignement et de recherche français ou étrangers, des laboratoires publics ou privés.

Orange peel coupling in multilayers with perpendicular magnetic anisotropy: Application to (Co/Pt)-based exchange-biased spin-valves

J. MORITZ, F. GARCIA, J. C. TOUSSAINT, B. DIENY(*) and J. P. NOZIÈRES
SPINTEC, CEA/Grenoble/DRFMC - 38054 Grenoble Cedex 9, France

(received 28 January 2003; accepted in final form 4 November 2003)

PACS. 75.70.-i – Magnetic properties of thin films, surfaces, and interfaces.

PACS. 75.30.Gw – Magnetic anisotropy.

PACS. 75.50.Ss – Magnetic recording materials.

Abstract. – Néel's theory of magnetostatic coupling between two magnetic layers with in-plane magnetization separated by a non-magnetic spacer has been extended to the case of multilayers with perpendicular anisotropy. It is shown that the presence of a correlated roughness between the successive interfaces induces an interlayer coupling through the spacer analogous to the well-known orange peel coupling. However, depending on the parameters describing the interfacial roughness, the magnetic anisotropy and the exchange stiffness constant, this coupling can favor either parallel or an antiparallel alignment of the magnetization in the two ferromagnetic layers. This model was used to quantitatively interpret the variation of interlayer coupling *vs.* thickness of Pt spacer layer in out-of-plane magnetized exchange-biased spin-valves comprising (Pt/Co) multilayers as free and pinned layers. It is shown that the net coupling can be interpreted by the coexistence of perpendicular orange peel and oscillatory RKKY couplings. Interestingly, since these two couplings have different thickness dependence, in certain range of Pt thickness, the coupling changes sign during growth, being antiferromagnetic at the early stage of the growth of the top (Co/Pt) multilayer but ferromagnetic once the growth is completed.

Introduction. – Néel first studied the magnetostatic coupling arising between two magnetic layers with in-plane magnetization separated by a non-magnetic spacer layer [1]. This so-called orange peel coupling is ferromagnetic when the successive interfaces present the same correlated in-phase waviness and decreases exponentially with spacer layer thickness. It is quite frequently observed in magnetic sandwiches and especially in spin-valves [2]. The observation of oscillatory interlayer coupling of RKKY-type associated with oscillations in giant magnetoresistance in magnetic multilayers [3] has launched a very strong interest for coupling phenomena in multilayers with in-plane anisotropy. The possibility of coexistence of several periods of oscillations in RKKY coupling was predicted by Bruno [4] and observed experimentally in (Fe/Cr) [5] and (Co/Cu) [6] wedge multilayers grown by molecular beam epitaxy. In contrast to in-plane magnetized systems, interlayer coupling in the presence of perpendicular anisotropy has been investigated in a very limited number of systems: Co/Au(111)/Co sandwiches [7, 8], (111)-(Co/Pt) superlattices [9], Co/Ir(111) multilayers [10]. Antiferromagnetic coupling coexisting with perpendicular anisotropy has been observed in some of these systems for particular ranges of spacer layer thickness. Surprisingly, the magnetostatic coupling which may arise in these perpendicularly magnetized systems in the presence of a correlated roughness has not been discussed so far, nor experimentally nor theoretically.

(*) E-mail: bdieny@cea.fr; dieny@drfmc.ceng.cea.fr

In this letter, we extend Néel's theory of magnetostatic coupling in magnetic multilayers to the case of multilayers with perpendicular anisotropy and use this new theory to quantitatively interpret the variation of coupling *vs.* Pt spacer layer thickness in spin-valves with perpendicular magnetic anisotropy. This letter is divided into two parts. The first part deals with the calculation of the so-called orange peel coupling in the presence of a perpendicular magnetic anisotropy. The second part reports an experimental study of interlayer coupling in perpendicular exchange-biased spin-valves in relationship with a structural characterization of the interfacial roughness.

Model. – We consider two ferromagnetic layers F_1 and F_2 of thickness t separated by a non-magnetic metallic layer (NM) of thickness b (see fig. 1). If F_1 and F_2 were uniformly magnetized along the direction perpendicular to the plane and assuming that the interfaces were perfectly flat, then the magnetostatic energy of the system would be independent of the relative orientation of \mathbf{M}_1 and \mathbf{M}_2 , where \mathbf{M}_1 and \mathbf{M}_2 are the magnetization of F_1 and F_2 , respectively. This is not the case when the interfaces are wavy. As in Néel's model of orange peel coupling, we assume that the roughness of the F_1 and F_2 interfaces are correlated (in-phase) and can be described by a cosine waviness

$$z = h \cos\left(\frac{2\pi x}{T}\right) \quad (1)$$

as depicted in fig. 1. $2h$ and T , respectively, represent the peak-to-peak amplitude of the roughness and its wavelength. We then define θ as the angle between the normal to the interface and the z -direction. In most experimental situations, $T \gg h$ so that θ takes the simple form

$$\theta(x) = hp \cos px, \quad (2)$$

where $p = \frac{2\pi}{T}$. The magnetization in each layer is assumed to be submitted to a perpendicular anisotropy large enough to counterbalance the easy-plane shape anisotropy. Since we are dealing with multilayers comprising very thin magnetic layers (for instance, (Pt 2 nm/Co 0.4 nm)₄), we assume that the dominant anisotropy term is the interfacial anisotropy and that the local anisotropy axis always points along the normal to the interfaces. Due to the perpendicular anisotropy, the magnetization is in average perpendicular to plane. However, due to the misalignment of the anisotropy axes caused by the interfacial waviness, the magnetization spatially oscillates. At first order in Fourier transform, the local magnetization can be described by $\psi(x) = \psi_0 \cos px$, where ψ is the angle between the direction of the magnetization and the z -direction. The parameter ψ_0 represents the amplitude of the magnetization fluctuations. It must be calculated by minimizing the total energy of the system. The two situations of parallel and antiparallel alignments of the averaged magnetization in the two magnetic layers are considered. These two situations are described by assuming that the average magnetization of one layer remains fixed (\mathbf{M}_1), whereas the magnetization of the other is $\varepsilon\mathbf{M}_2$ with $\varepsilon = 1$ or -1 . Considering all these assumptions, the different energy terms can be calculated analytically to the second order in ψ_0 . These terms are the exchange within each magnetic layer, the anisotropy at each interface and the magnetostatic energies.

The exchange energy takes the simple form

$$E_{ex} = \frac{2t}{T} \int_0^T A \left(\frac{\partial\psi}{\partial x}\right)^2 dx = At p^2 \psi_0^2, \quad (3)$$

where A is the exchange constant.

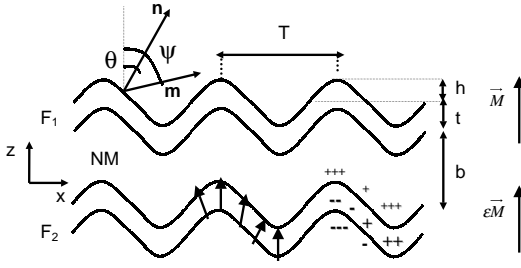


Fig. 1

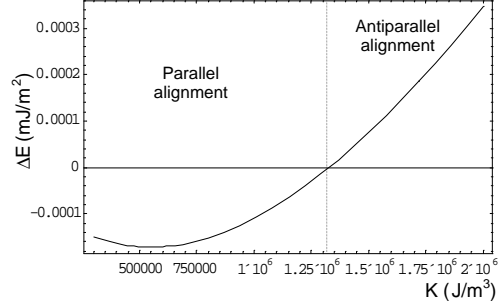


Fig. 2

Fig. 1 – Schematic representation of a magnetic trilayer consisting of two ferromagnetic layers (F_1 and F_2) separated by a non-magnetic spacer (NM). The positive and negative signs represent the interfacial charges and the volume charges (assumed to be located in the middle of the ferromagnetic layers).

Fig. 2 – Variation of the coupling with the anisotropy constant. The structural and magnetic parameters used for the calculations are $M_s = 1.4 \times 10^6$ A/m; $A = 10^{-11}$ J/m; $h = 2$ nm; $T = 8$ nm; $b = 4$ nm; $t = 0.5$ nm.

Following the assumption that the anisotropy axis is always locally normal to the interface, the anisotropy energy at each interface can be written

$$E_{\text{ani}} = -\frac{2t}{T} \int_0^T \cos^2(\theta(x) - \psi(x)) dx = Kt(hp - \psi_0)^2 = Kt(\theta_0 - \psi_0)^2, \quad (4)$$

where K is the uniaxial anisotropy constant.

To calculate the magnetostatic energy, we consider separately the magnetic charges at the interfaces and in the bulk of the magnetic layers (see fig. 1). The interfacial density of charges is given by

$$\sigma_s = \vec{m} \cdot \vec{n} = Ms \cos[(\theta_0 - \psi_0) \cos px] \approx \sigma_0 - \sigma_1 \cos 2px \quad (5)$$

with $\sigma_0 = Ms[1 - \frac{(\theta_0 - \psi_0)^2}{4}]$ and $\sigma_1 = \frac{Ms}{4}(\theta_0 - \psi_0)^2$.

The volume charges are proportional to the divergence of the magnetization which varies only along the x -direction (see fig. 1). Since the magnetic layers are very thin, the bulk charges can be considered as a surface charge density concentrated on a single plane in the middle of the magnetic layer. The corresponding density of charges is

$$\sigma_v = \sigma_2 \sin px \quad \text{with} \quad \sigma_2 = pMs\psi_0 t. \quad (6)$$

It is interesting to note that the interfacial and bulk densities of charges do not oscillate with the same wavelength.

As in Néel's model of orange peel coupling, the various density of charges listed above are supposed to lie on flat surfaces. The magnetostatic potential V generated by these surface charge densities is calculated by solving the Laplace equation $\Delta V = 0$. Using the boundary condition $\frac{\partial V}{\partial z}|_{Ii+} - \frac{\partial V}{\partial z}|_{Ii-} = -\sigma(x)$ and since all charge densities are of cosine form, the magnetic potential induced by the surface and volume charges are, respectively,

$$V_s = -\frac{\sigma_0}{2}|z| - \frac{\sigma_1}{4p} \cos 2px \exp[-2p|z|] \quad (7)$$

and

$$V_v = \frac{\sigma_2}{2p} \sin px \exp[-p|z|]. \quad (8)$$

In these expressions, the origin of the z -axis is taken at the intercept of the z -axis with the plane of charges.

The magnetostatic energy is then deduced from the expressions (5)-(8) by the relationship

$$E = \frac{\mu_0}{2} \frac{1}{T} \int_0^T \sum_i \sum_j V_i(x, z_j) \sigma_j(x) dx, \quad (9)$$

where $V_i(x, z_j)$ is the potential created by the surface charge density i on the surface charge density $\sigma_j(x)$ located at surface j . The summation of all the different terms yields the magnetostatic energy

$$E_{\text{mag}} = \frac{\mu_0}{2} \left[-\varepsilon \frac{\sigma_1^2}{8p} \exp[-2pb] [1 - \exp[-2pt]]^2 + \varepsilon \frac{\sigma_2^2}{4p} \exp[-p(b+t)] + \sigma_0^2 t - \frac{\sigma_1^2}{4p} \exp[-2pt] \right]. \quad (10)$$

The total energy is the sum of the anisotropy, exchange and magnetostatic energies. It is then minimized with respect to ψ_0 in parallel and antiparallel magnetic configurations. The minimization yields the equilibrium magnetic distortion $\psi_{0,s=\pm 1}$ and energy in both configurations. The resulting coupling is then given by

$$\Delta E = E_{\text{tot}}(\psi_{0,\varepsilon=1}) - E_{\text{tot}}(\psi_{0,\varepsilon=-1}).$$

The sign of ΔE determines whether the coupling favors a parallel ($\Delta E < 0$) or an antiparallel ($\Delta E > 0$) alignment of the magnetizations of the two ferromagnetic layers.

We now examine the dependence of this coupling on the amplitude of the uniaxial perpendicular anisotropy. Choosing a set of structural and magnetic parameters for the magnetic and the spacer layers corresponding to Co sputtered layers (see caption of fig. 2), the coupling can be plotted as a function of the anisotropy constant (fig. 2). For low values of the anisotropy constant, the coupling is negative, which means that parallel alignment of the magnetizations is favored. When the anisotropy constant is larger than 1.32×10^6 J/m³, the coupling favors an antiparallel alignment of the magnetizations. We calculated also that the magnetic distortion ψ_0 follows the same variation in sign than the coupling.

In order to understand why the coupling can favor parallel or antiparallel alignment, we consider two extreme cases: For very low-anisotropy amplitudes, the magnetization remains uniformly parallel to the z -axis as illustrated in fig. 3a in order to minimize the surface charges and because of the exchange stiffness. In this case, there are no volume charges because the magnetization is almost uniform within each layer. As a result, the dominant magnetostatic interaction is the interaction between the charge densities which are facing each other at the F₁/NM and NM/F₂ interfaces. Since these charge densities are opposite in parallel magnetic configuration, parallel alignment is favored in this case. This situation corresponds to a negative value of ψ_0 . When the anisotropy is large, the magnetization follows the normal to the interface as shown in fig. 3b. Here, the interfaces are uniformly charged and generate no coupling. But a large oscillatory distribution of volume charges arise due to the divergence of the magnetization in the x -direction. For parallel magnetic alignment, the volume charges oscillate in phase in F₁ and F₂ which is unfavorable from a magnetostatic point of view since charges of the same sign are facing each other. Consequently, this situation favors an antiparallel alignment of the magnetizations. The sign of ψ_0 is here positive which allows to reduce the anisotropy energy. In the limit of very large anisotropy, the distortion ψ_0 becomes equal to θ_0 meaning that the magnetization always points along the normal to the interface.

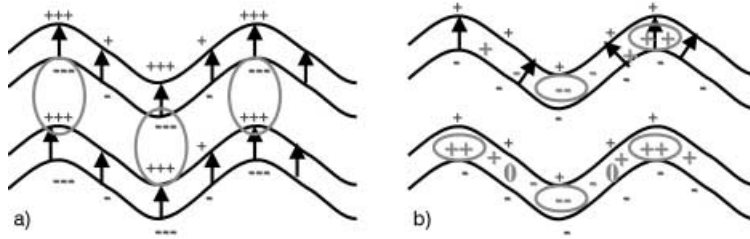


Fig. 3 – a) Schematic representation of the magnetization in the case of low anisotropy. The average magnetization being parallel to the z -axis, magnetic charges of opposite signs appear on the interfaces generating a parallel coupling. b) In the case of large anisotropy, the magnetization follows the normal to the surface. The volume charges of the same sign in the magnetic layers generate an antiparallel coupling.

Experiments. – In order to test experimentally our model, we prepared a series of spin-valves with perpendicular magnetization of the composition: $(\text{Pt } 2 \text{ nm}/\text{Co } 0.4 \text{ nm})_4/\text{Pt } t_{\text{Pt}}/(\text{Co } 0.4 \text{ nm}/\text{Pt } 2 \text{ nm})_3/\text{Co } 0.4 \text{ nm}/\text{PtMn } 7.5 \text{ nm}$. The samples were deposited onto Si/SiO_2 substrates by magnetron sputtering at room temperature. More details on the experimental procedure were published in ref. [11]. The measurement of the hysteresis loops were performed by extraordinary Hall effect at room temperature [12, 13]. The inset of fig. 4 shows the hysteresis loop of a spin-valve with a 3 nm thick spacer. The field was applied perpendicular to the plane. Two separated hysteresis loops can be clearly identified. The top multilayer which is exchange-biased by FeMn exhibits a shifted hysteresis loop with a bias field of 90 Oe. The free layer also presents a shifted loop but with a much weaker bias which depends on the spacer thickness. As for in-plane spin-valves, this latter loop shift provides a measurement of the interlayer coupling through the spacer layer.

Result and discussion. – Figure 4 presents the variation of the strength of the coupling *vs.* spacer thickness. The error bars on the spacer thickness axis correspond to one atomic plane

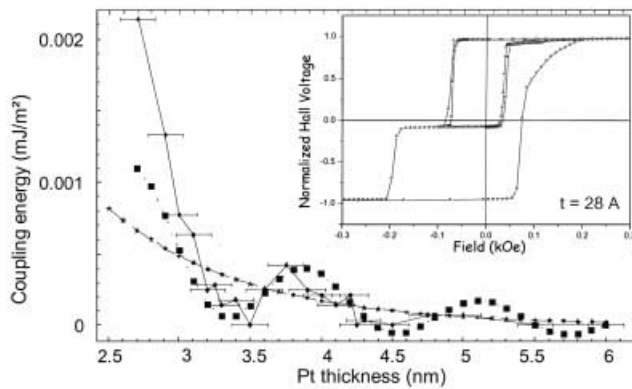


Fig. 4 – Variation of the experimental coupling with the spacer thickness (square). Fit obtained with the orange peel model (dashed line). Fit obtained by adding the contributions from the orange peel and RKKY coupling (dotted line). Inset: major and minor hysteresis loops of the sample $(\text{Pt } 2 \text{ nm}/\text{Co } 0.4 \text{ nm})_4/\text{Pt } t_{\text{Pt}}/(\text{Co } 0.4 \text{ nm}/\text{Pt } 2 \text{ nm})_3/\text{Co } 0.4 \text{ nm}/\text{PtMn } 7.5 \text{ nm}$ measured by extraordinary Hall effect. The two steps are attributed to the pinned and the free multilayers. The coupling field is accurately determined by the measurement of the shift of the free-layer minor loop.

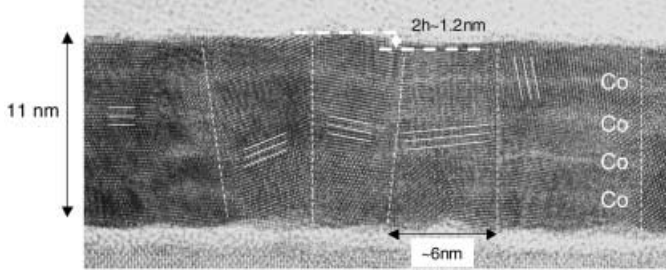


Fig. 5 – Cross-sectional view of a multilayer of composition $(\text{Pt } 1.8/\text{Co } 0.5)_4/\text{Pt } 1.8$ obtained by transmission electron microscopy. The waviness determined from the observation is 6 nm for the wavelength and 1.2 nm for the peak-to-peak amplitude.

of Pt. The coupling is found to be parallel for all spacer thickness b and rapidly decreases as b increases. The decrease, however, is not monotonous and an oscillatory behavior is observed with local maxima in the coupling amplitude around 3.8 and 5 nm. In order to determine the roughness parameter to input in the model, cross-sectional transmission electron-microscopy observations were performed on these samples (see fig. 5). As commonly observed in sputtered samples, these systems have a columnar texture. This texture is characterized by a grain size of about 6 nm and an interfacial peak-to-peak waviness of 1.2 nm. We therefore set $T = 6$ nm; $h = 0.6$ nm in the model. We then used our above calculation to fit the experimental coupling variation and plotted the result in fig. 4. The parameters of the fit are: $A = 0.28 \times 10^{-11}$ J/m; $K = 2.5 \times 10^6$ J/m³; $M = 1.4 \times 10^6$ A/m. The anisotropy constant was chosen equal to the experimental value determined in our multilayers by measuring the saturation field with in-plane applied field.

The orange peel mechanism allows to reproduce the average decrease of the coupling with increasing spacer layer thickness but not the oscillatory behavior. Therefore, we introduced a second component in the coupling which is of RKKY-type. Following the simple formulation of Yafet [14], the RKKY coupling takes the form

$$E_{\text{RKKY}} = -I_0 \frac{d^2}{b^2} \sin(2kb),$$

where I_0 is the exchange parameter, d the interatomic distance within the spacer in the z -direction and k is a wave vector related to the shape of the Fermi surface in the growth direction. Adding the two different contributions to the coupling, we were able to fit the experimental data including the oscillatory behavior. This is shown in fig. 4. Adjusting the wave vector to fit the oscillation leads to a wavelength of 1.2 nm and an exchange constant I_0 of 0.062 mJ/m². At large Pt thickness ($t_{\text{Pt}} > 5$ nm), the oscillations however decrease faster experimentally than in the fit. This can be ascribed to some degree of uncorrelated roughness in the stack which results in a distribution of spacer layer thickness. The latter can lead to a smearing of the oscillations at large spacer thickness.

The above interpretation of the coupling variation in terms of coexistence of RKKY and orange peel coupling is supported by some of our previously published results on exchange-biased perpendicular spin-valves [11]. We observed that in the range of thickness corresponding to the local minimum of interlayer coupling (around 3.5 nm of Pt), the virgin magnetic state of the system was an antiparallel alignment between the magnetization in the two ferromagnetic multilayers. In contrast, around a Pt thickness of 3.8 nm, the initial magnetization was equal to the saturation magnetization indicating a parallel magnetic alignment. However, as observed in the present study, the shift of the minor loop of the free layer indicates that

the interlayer coupling is always parallel in the completed structures whatever the Pt spacer thickness. These observations can be interpreted as follows: The amplitude of the orange peel coupling increases with the thickness of the ferromagnetic layers. As a result, the RKKY coupling is dominant in the initial stage of the growth of the top (Co/Pt) multilayer so that its magnetization nucleates in the direction determined by the sign of the coupling. As the growth proceeds, the orange peel coupling which is parallel in these systems plays a larger and larger role so that, finally, in the completed structures, it dominates the RKKY coupling.

Conclusion. – By extending Néel’s theory of orange peel coupling to multilayers with perpendicular anisotropy, we showed that the magnetostatic interaction between two perpendicularly magnetized layers in the presence of a correlated roughness can favor either a parallel or an antiparallel magnetic alignment of the magnetization in these two layers. The sign of the coupling results from an interplay between the magnetostatic, the exchange and the anisotropy energy. As for systems with in-plane magnetization, its amplitude depends on the structural characteristics of the layers (grain size and roughness) as well as on the spacer and magnetic layer thickness. The application of this model to exchange-bias perpendicular spin-valves indicated a coexistence between orange peel and RKKY-type coupling. In our samples, the perpendicular orange peel coupling was found to favor parallel alignment. Further experimental work is in progress in order to quantitatively investigate the influence of roughness on the interlayer coupling and in particular observe the regime in which antiparallel alignment is favored [15].

* * *

This work was supported by Région Rhône Alpes. We acknowledge P. BAYLE GUILLEMAUD for the TEM observation in fig. 5.

REFERENCES

- [1] NÉEL L., *Cr. Hebd. Acad. Sci.*, **255** (1962) 1676.
- [2] DIENY B., SPERIOSU V. S., PARKIN S. S. P., GURNEY B. A., WILHOIT D. R. and MAURI D., *Phys. Rev. B*, **43** (1991) 1297.
- [3] PARKIN S. S. P., MORE N. and ROCHE K. P., *Phys. Rev. Lett.*, **64** (1990) 2302.
- [4] BRUNO P. and CHAPPERT C., *Phys. Rev. Lett.*, **67** (1991) 1602.
- [5] UNGURIS J., CELOTTA R. J. and PIERCE D. T., *Phys. Rev. Lett.*, **67** (1991) 140.
- [6] BLOEMEN P. J. H., JOHNSON M. T., VAN DE VORST M. T. H., COEHOORN R., DE VRIES J. J., JUNGBLUT R., AAN DE STEGGE J., REINDERS A. and DE JONGE W. J. M., *Phys. Rev. Lett.*, **72** (1994) 764.
- [7] GROLIER V. *et al.*, *Phys. Rev. Lett.*, **71** (1993) 3023.
- [8] DE VRIES J. J., BLOEMEN P. J. H., JOHNSON M. T., AAN DE STEGGE J., REINDERS A. and DE JONGE W. J. M., *J. Magn. & Magn. Mater.*, **129** (1994) L124.
- [9] LE DANG K., VEILLET P., CHAPPERT C., FARROW R. F. C., MARKS R. F., WELLER D. and CEBOLLADA A., *Phys. Rev. B*, **50** (1994) 200.
- [10] ITOH H., YANAGIHARA H., SUZUKI K. and KITA E., to be published.
- [11] GARCIA F., MORITZ J., ERNULT F., AUFFRET S., RODMACQ B., DIENY B., CAMARERO J., PENNEC Y., PIZZINI S. and VOGEL J., *IEEE Trans. Magn.*, **38** (2002) 2730.
- [12] CANEDY C. L., LI X. W. and XIAO G., *J. Appl. Phys.*, **81** (1997) 5367.
- [13] ZHANG S., *Phys. Rev. B*, **51** (1995) 3632.
- [14] YAFET Y., *Phys. Rev. B*, **36** (1987) 3948.
- [15] We did observe antiferromagnetic orange peel coupling in very recent experiments performed with different spacer layer. These results will be published in a separate paper.